Bull. Mater. Sci., Vol. 40, No. 1, February 2017, pp. 101–106. © Indian Academy of Sciences.
DOI 10.1007/s12034-016-1350-4

Influence of oxidant and fuel on the powder characteristics of $LiNbO_3$ synthesized by combustion method

D H PIVA, H BIZ, R H PIVA and M R MORELLI*
Laboratory of Ceramic Synthesis and Formulation, Materials Engineering Department, PPG-CEM, Federal University of São Carlos, 13565-905 São Carlos, Brazil

MS received 6 November 2015; accepted 9 June 2016

Abstract. **Lithium niobate ($LiNbO_3$) is widely recognized as a promising material for replacing lead-based piezoelectric ceramics. Although the $LiNbO_3$ synthesis by combustion method has been investigated with particular attention recently, the influence of oxidants and different fuels' sources on the synthesized powders has not yet been thoroughly studied. In this work we investigate the influence of urea and maleic hydrazide as fuels and ammonium nitrate as an oxidant on the powder characteristics of $LiNbO_3$ synthesized by combustion method. In addition, powder characteristics and sinterability of powders prepared by combustion method are compared with those of powders prepared by solid-state reaction. The results show that the second phase $LiNb_3O_8$ was detected only when an oxidant agent was used in the synthesis process. Among all combustion reactions, the powders prepared with excess of urea presented better final characteristics. As a result, the sintering temperature for $LiNbO_3$ powders prepared by combustion method was appreciably lowered when compared with those prepared by solid-state reaction.**

Keywords. **Combustion synthesis; $LiNbO_3$; lithium niobate; solid-state reaction; sintering.**

1. Introduction

Alkaline niobates are one of the most promising candidates to replace the widely used lead-based piezoelectric ceramics [1]. Among the alkaline niobates family, lithium niobate ($LiNbO_3$) has been extensively investigated due to its very interesting and improved ferroelectric, pyroelectric, piezoelectric and electro-optical properties [2]. Of particular interest, $LiNbO_3$ has found applications in nonlinear optics, thin-film capacitors, pyroelectric detectors, optical memories and electro-optical modulators [1,3]. Most of these applications demand the production of $LiNbO_3$ as single crystal or thin films, although polycrystalline $LiNbO_3$ ceramics also have some important technological applications. However, the main drawback in producing dense polycrystalline alkaline niobates is their poor sinterability and volatility of the alkaline constituents at high sintering temperatures. The efforts to address these issues have focused on the addition of some sintering aids [4,5] and sintering techniques [6,7]. A more promising approach used to facilitate densification is the reduction of the sintering temperature under the selection of appropriate synthesis methods that yields nanosized, high-surface-area and non-agglomerated powders [8].

The $LiNbO_3$ powders are commonly synthesized by solid-state reaction using lithium carbonate and niobium pentoxide as precursors. A serious weakness with this route is the high temperatures and long reaction times often required to produce single-phase powders. To overcome this problem several alternative methods have been applied to synthesize $LiNbO_3$ powders, including sol–gel, hydrothermal synthesis, molten salt method, peroxide route and combustion synthesis [9–20]. Among these techniques, the latter method yields single-phase and homogeneous powders in an extremely short period of time, at a low cost and with simple equipment [9,11]. The combustion synthesis involves a self-sustained reaction between the reactive specimens and the fuel. The reaction converts the initial mixture to a fine powder already crystallized as the desired compound [21]. Up to now, several works have been published regarding this method for the preparation of $LiNbO_3$ powders. With respect to the precursors, Liu and Xue [22] reported the effect of the different urea/(Nb_2O_5+Li_2CO_3) ratios in the synthesis of $LiNbO_3$ powder. Simultaneously, Liu *et al* [9] reported synthesis of $LiNbO_3$ using $Nb_2O_5 \cdot nH_2O$ as the source of niobium oxide. Although both the aforementioned works were carried out with urea as the fuel, a complementary report of Kuo *et al* [23] contains useful information related to the synthesis of nanocrystalline $LiNbO_3$ powders using glycine as the fuel. The investigation of different fuel agents is based on the fact that some new interaction can occur with the precursors and thus alter the characteristics of the synthesized powders. Depending on the amount of heat generated during the synthesis, it is possible to obtain better results regarding the crystallinity of the synthesized powders. However, despite several works showing the characteristic of $LiNbO_3$ powders prepared by combustion synthesis using urea and glycine as fuels, few studies were reported investigating the influence of hydrazine-based fuels and oxidants addition in the combustion synthesis of $LiNbO_3$.

*Author for correspondence (morelli@ufscar.br)

In this context, we report here the synthesis of $LiNbO_3$ powders by combustion method using urea and maleic hydrazide as fuels and ammonium nitrate as an extra oxidant source. In addition, the sinterability and characteristics of the powders obtained by combustion method were compared to powders synthesized by solid-state reaction. The powders and the sintered polycrystalline samples were characterized by a series of techniques, including X-ray diffraction (XRD), scanning electron microscopy (SEM) and dilatometry.

2. Experimental

2.1 *Materials*

Ammonium niobate oxalate hydrate ($NH_4H_2[NbO(C_2O_4)_3]\cdot 3H_2O$, CBMM, 97%, referred to as ANO), lithium nitrate ($LiNO_3$, Nuclear, 95%), urea ($CO(NH_2)_2$, Synth, 99.5%), ammonium nitrate (NH_4NO_3, Merck, 99%) and maleic hydrazide ($C_4H_4N_2O_2$, Avocado Research Chemicals, 97%) were used as precursors for $LiNbO_3$ powders prepared via a combustion method, whereas niobium oxide (Nb_2O_5, CBMM, 99.8%) and lithium carbonate (Li_2CO_3, Carlo Erba, 99%) were used as precursors in the synthesis of $LiNbO_3$ powders by solid-state reaction. All chemicals were used as received.

2.2 *Synthesis of $LiNbO_3$ powders via combustion method*

In order to evaluate the effect of urea and oxidant content on the $LiNbO_3$ powder characteristics, four samples were prepared with different reactant ratios, as shown in table 1. Urea and maleic hydrazide contents used in the R1 and R4 reactions were calculated according to the salt-to-fuel ratio proposed by Jain *et al* [24]. The amount of urea used in the R2 reaction was based on the data reported in the literature [25], which presented the maximum fuel ratio that should be used to avoid the production of ash in the final product. Finally, the amount of 5 mol of NH_4NO_3 used in the R3 reaction was adopted considering previous analyses in our laboratory, presenting in this case a greater glowing effect and an explosive reaction with superior release of gases. The excess of urea used in this reaction was calculated to allow the decomposition of the extra oxidant added.

In the synthesis of powders, proper amounts of $LiNO_3$ and ANO were dissolved in deionized water to obtain a solution containing a niobium-to-lithium ions ratio of 1:1. Following this, the calculated amounts of fuels and oxidants (as in table 1) were added to the aforementioned precursor solution, and the mixture was stirred to obtain a clear and homogeneous solution. Afterward, the solution was transferred to a porcelain crucible, and then heated up to 300°C on a hot plate to promote the evaporation of water and the initiation of the combustion reaction. Subsequently, the crucible was quickly transferred to a furnace pre-heated at 600°C, where the combustion reaction completely took place. The temperature in all steps of the combustion reactions was measured by thermal imaging using an infrared thermometer (Raytek, MA2CSFL).

To compare powder characteristics and sinterability, $LiNbO_3$ powders were prepared also by conventional solid-state reaction. In this case, stoichiometric amounts of Nb_2O_5 and Li_2CO_3 were homogenized in isopropanol and the mixture was ball-milled for 7 h. The suspension was dried at 110°C, and then crushed with a pestle in an agate mortar, sieved through a 100 μm sieve and finally calcined at 950°C for 2 h.

2.3 *Sample preparation and sintering*

Prior to the sample preparation, the $LiNbO_3$ powders synthesized by combustion method and solid-state reaction were ball-milled in ethanol for 7 h. The suspensions were dried at 110°C, and sieved through a 400 mesh. The powders were uniaxially compacted under 70 MPa and isostatically re-pressed under 200 MPa into pellets. Linear shrinkage was measured using a Netzsch 402 C dilatometer up to 1100°C at a heating rate of 5°C min^{-1}. The green bodies were sintered in air at temperatures between 950 and 1150°C for 1 h at a heating rate of 5°C min^{-1}.

2.4 *Characterization*

XRD measurements were performed on a Siemens D5000 powder X-ray diffractometer using Cu Kα radiation (λ = 1.54056 Å), and operating at 20 kV and 40 mA. Diffraction patterns were collected over the 2θ range of 5–80° at a stepped scan rate of 0.03° per step and a count time of 1 s per step. Nitrogen sorption isotherms were obtained at −196°C using a Micromeritics Gemini II 2370 instrument. The specific surface area (S_{BET}) was determined by the Brunauer–Emmett–Teller method at p/p_0 = 0.05–0.2. Particle size

Table 1. Solution combustion synthesis of $LiNbO_3$ powders.

	Molar ratio				
Reaction	$LiNO_3$	$NH_4H_2[NbO(C_2O_4)_3]\cdot 3H_2O$	$CO(NH_2)_2$	$C_4H_4N_2O_2$	NH_4NO_3
R1 (stoichiometric urea)	1	1	0.67	—	—
R2 (extra urea)	1	1	8.37	—	—
R3 (with ammonium nitrate)	1	1	2.67	—	5
R4 (stoichiometric hydrazide)	1	1	—	0.25	—

distribution was measured using a Sedigraph 5000 D equipment (Micromeritics). The particle morphology and the microstructure of the sintered samples were examined by SEM (Leica Cambridge Stereoscan 440) at an acceleration voltage of 20 kV. For the SEM analysis, the sintered samples were ground using 600 and 1200 grit SiC papers followed by final polishing with alumina suspension (1 and 0.3 μm), and then thermally etched. The relative density of the sintered samples was determined using Archimedes' principle with water as the immersion medium. The theoretical density of $LiNbO_3$ used was 4.64 g cm^{-3}.

3. Results and discussion

3.1 *Combustion synthesis*

Initially, several samples were prepared via combustion synthesis using different metal salt–fuel–oxidant ratios. Figure 1 shows the temperature evolution and a series of successive digital images recorded during different stages for selected combustion reactions. When stoichiometric urea is used (R1), the temperature increases quickly up to 840°C as the combustion reaction occurs, and then slowly decreases as the combustion reaction proceeds. A smoldering flame can be observed in the images for the R1 reaction, which was similar to the R2 reaction (not shown), although the latter exhibited a lower and constant temperature of 775°C during the whole synthesis time. Regarding the sample prepared by the reaction containing NH_4NO_3 as oxidant (R3), the temperature abruptly increases upon the ignition of the combustion, and the maximum combustion temperature reaches 930°C. A flaming-type reaction took place as can be seen in the digital images during the reaction (figure 1 insets). The combustion reaction observed in reaction R3 was so far the most exothermal in nature, whereas it is reasonable to assume that this phenomenon results from the violent combustion of the NH_4NO_3 as an extra oxidant agent [26]. The combustion reaction observed while using maleic hydrazide (R4) is very close to that of R3. However, despite its lower temperature, the ignition of the combustion process in R3 occurs quickly, yielding a short reaction time.

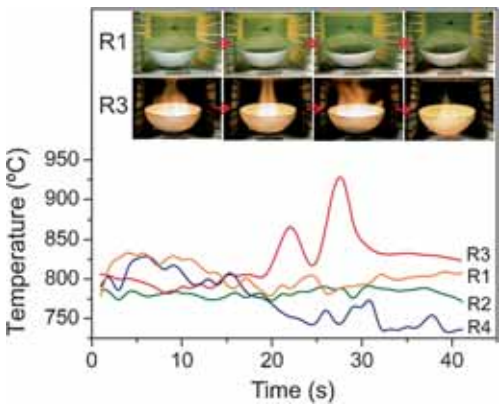

Figure 1. Temperature against time during the different stages of the combustion reaction. The insets show a sequence of digital images recorded during the combustion.

3.2 *Phase characterization and morphology of the $LiNbO_3$ powders*

The XRD patterns shown in figure 2 indicate the formation of the hexagonal $LiNbO_3$ phase (JCPDS No. 20-0631) in the powders synthesized by the combustion reactions R1 and R2. In addition, no occurrence of secondary phases or evidence of unreacted precursors was observed in these reactions. Note that a clear increase in the intensity of the diffraction peaks is observed for the sample prepared by reaction R2, demonstrating that the crystallinity of the synthesized powder is improved when excess of urea is used. In contrast to the single-phase powders produced by the R1 and R2 reactions, the undesirable $LiNb_3O_8$ phase (JCPDS No. 36-0307) was detected in the XRD patterns of the powders prepared by R3 and R4 reactions. Liu *et al* [9] attribute the formation of $LiNb_3O_8$ phase to the high temperature reachedduring the reaction. A similar result was observed by Kamali and Fray [10] by increasing the temperature of the thermal treatment. Both authors have attributed the $LiNb_3O_8$ phase formation to lithium volatilization during heat treatment. It is noteworthy that the excess of lithium has been used to compensate the lithium loss of Li-containing compounds during the combustion synthesis [27]. In addition, according to Jardiel *et al* [28] a rapid quenching from the high temperature can prevent the reversible formation of $LiNb_3O_8$ secondary phase on cooling. Therefore, the high temperature during the reaction R3 and the lower cooling rate during the reaction R4 (figure 1) may be responsible for the formation of $LiNb_3O_8$. From the XRD pattern (figure 2), it can be inferred that the combustion reaction containing only urea as fuel (R1 and R2) is the most appropriate one for synthesis of single-phase $LiNbO_3$.

Figure 3 shows the morphology of all synthesized powders by combustion method. It can be observed that each reaction yields homogeneous powders. However, the R1, R2 and R4 reactions produced highly agglomerated powders. This fact is due to the high temperature achieved during the

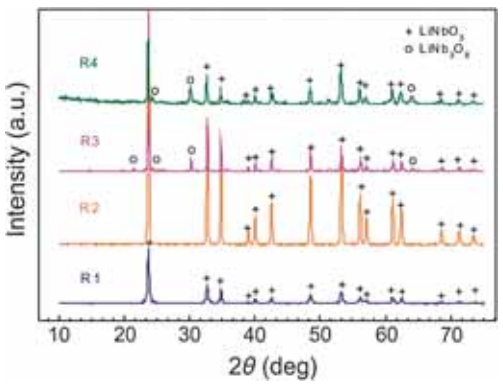

Figure 2. XRD patterns of the $LiNbO_3$ powders synthesized in the different combustion reactions.

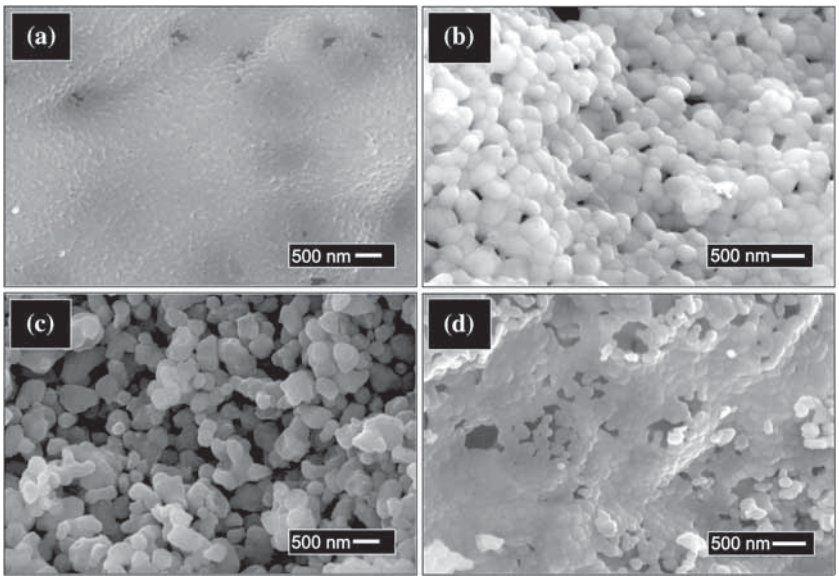

Figure 3. SEM micrographs of $LiNbO_3$ powders synthesized by combustion reactions (**a**) R1, (**b**) R2, (**c**) R3 and (**d**) R4.

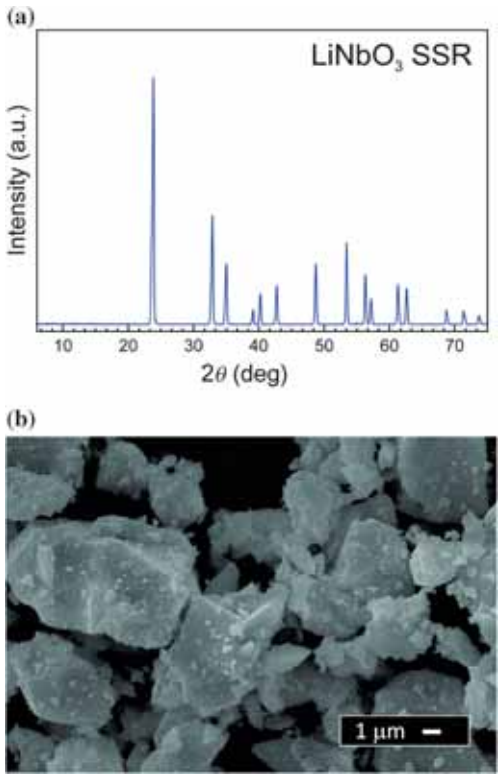

Figure 4. (**a**) XRD pattern of the $LiNbO_3$ powder synthesized by solid-state reaction and (**b**) SEM image of the powder.

combustion in these reactions, thereby promoting particles interaction in the initial sintering stage. The large particle size for the powder synthesized by the R2 reaction may be related to the long time to burn out the fuel. This grain growth phenomenon at high combustion temperature has been previously reported by Zeng and Tung [14]. The powder produced by R3 apparently had the lowest degree of agglomeration, although it has been produced by the combustion synthesis at higher temperature (see figure 1). This result is explained in terms of the addition of NH_4NO_3, which results in the generation of a large volume of gases during the decomposition. According to Mokkelbost *et al* [13], the large amount of gaseous products generated during the combustion synthesis reduces the contact between adjacent particles; therefore, it prevents bond formation and consequently agglomeration of particles.

From the previous results, better characteristics of the $LiNbO_3$ powders such as high crystallinity, absence of second phases and low degree of agglomeration were achieved by combustion synthesis using urea in excess (R2). Considering these good powder characteristics, the sintering studies will be focused on the powder synthesized by the R2 reaction (hereafter designated as $LiNbO_3$ R2), and will be compared with the powder obtained by solid-state reaction (designated as $LiNbO_3$ SSR). Prior to the sintering studies, the crystal structure of the $LiNbO_3$ SSR was examined by XRD as shown in figure 4a, confirming the existence of hexagonal $LiNbO_3$ as in the powders synthesized by combustion. Also, the diffraction pattern shows that the powder is highly crystalline. The surface morphology of the particles is shown in figure 4b. It can be observed that the powder is composed of large and highly densified agglomerates.

3.3 *Milling the $LiNbO_3$ particles*

The effect of milling on the $LiNbO_3$ powders is shown in figure 5. From the plots, it is clear that a milling step can be used to reduce the average particle size along with a narrow size distribution in both $LiNbO_3$ SSR and $LiNbO_3$ R2 powders. Taking the d_{50} value as a parameter, it has been found

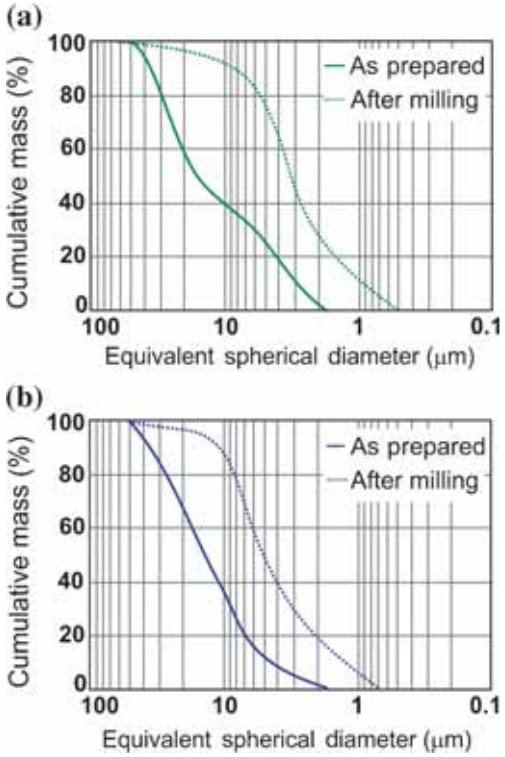

Figure 5. Particle size distribution of the powders: (**a**) $LiNbO_3$ R2 and (**b**) $LiNbO_3$ SSR.

Table 2. Specific surface area before and after milling the $LiNbO_3$ powders prepared via combustion method and the solid-state reaction.

Samples	As prepared ($m^2\ g^{-1}$)	Milled ($m^2\ g^{-1}$)
$LiNbO_3$ R2	2.54	5.62
$LiNbO_3$ SSR	1.40	3.17

that the $LiNbO_3$ SSR powder is less susceptible to particle size reduction when compared with the $LiNbO_3$ R2 powder. In terms of values, the former exhibited a particle size reduction from 14.5 to 5.0 μm whereas the latter showed a significant reduction from 17.4 to 3.2 μm. The S_{BET} values shown in table 2 confirm the superior quality of the powder synthesized by combustion method.

3.4 *Sintering of the specimens*

Comparative dilatometric curves for samples prepared using the ball-milled powders synthesized by combustion method and solid-state reaction are shown in figure 6. The shrinkage starts at 800 and 900°C for the $LiNbO_3$ R2 and $LiNbO_3$ SSR samples, respectively. According to the dilatometric curves, it can be seen that the $LiNbO_3$ R2 powder showed a significantly higher sinterability compared with those of $LiNbO_3$ SSR. Since low-surface-area powders tend to possess inferior sintering behaviour, it is not surprising that the $LiNbO_3$

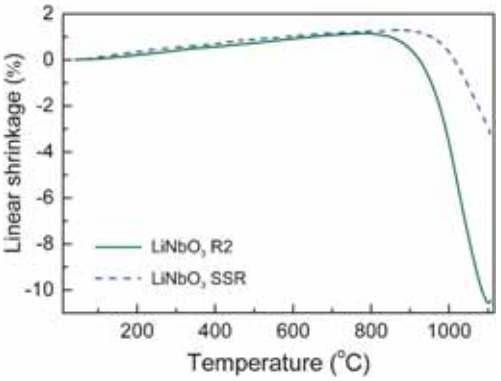

Figure 6. Dilatometric curves of the $LiNbO_3$ green pellets.

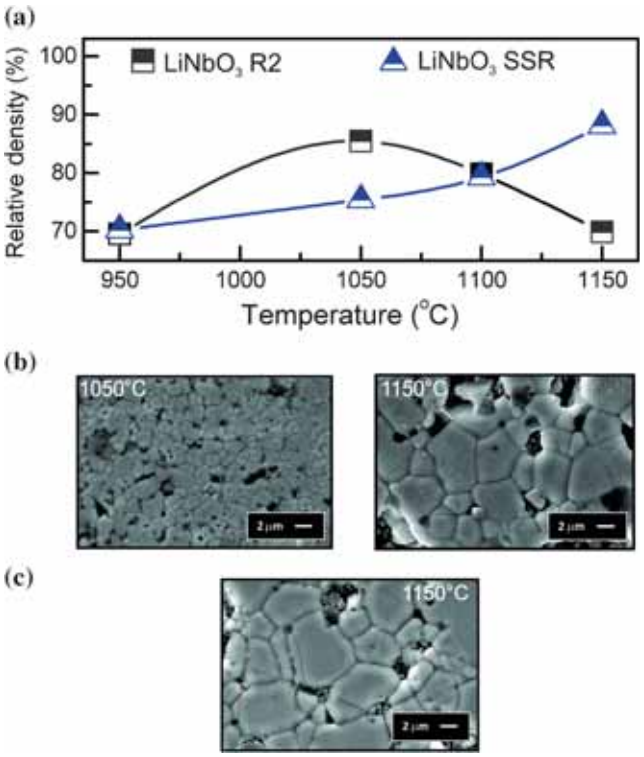

Figure 7. (**a**) Comparative densification curves for powders synthesized by combustion method and solid-state reaction. SEM micrographs are presented for (**b**) $LiNbO_3$ R2 at 1050 and 1150°C and (**c**) $LiNbO_3$ SSR polycrystalline samples at 1150°C.

SSR powders showed a higher temperature at which the sintering phenomenon starts, which is a consequence of the smallest S_{BET} value while synthesizing $LiNbO_3$ powders by solid-state reaction (see table 2).

Some selected SEM micrographs and the densification curves generated by the sintering studies are shown in figure 7. It can be seen that even starting from the same green densities of 62%, the sintered sample from $LiNbO_3$ R2 powder exhibits a greater relative density at a lower temperature than the sample prepared from $LiNbO_3$ SSR powder and indeed matches well with the previous dilatometric results (figure 6). A gradual reduction in densification over 1050°C

was observed for the $LiNbO_3$ R2 sample, reaching relative density value as low as 70% at 1150°C. A microstructural investigation of the $LiNbO_3$ R2 sintered sample from the SEM images presented in figure 7b shows a homogeneous fine-grained microstructure with uniform grains, averaging 1.5 μm in size at 1050°C. Moreover, the porosity is exclusively observed along intergranular locations at this temperature. Raising the sintering temperature to 1150°C for the $LiNbO_3$ R2 powder showed an abrupt reduction in the relative density of the polycrystalline sample. Furthermore, the grain size was greatly affected by the temperature, reaching a value almost three times higher when the temperature is raised from 1050 to 1150°C for the powder synthesized by combustion. The residual porosity considerably changes in number and size due to a higher grain coarsening already reported for the $LiNbO_3$ phase at high temperatures [29]. Regarding the densification of the $LiNbO_3$ SSR powders, it is possible to observe that it is much less reactive than those obtained by the combustion reaction. However, in a very similar way to the $LiNbO_3$ R2 powder, a high grain growth was also observed. Evidently the formation of the large grains is a direct effect of the increased grain-boundary motion when the temperature is raised [30].

4. Conclusion

$LiNbO_3$ powders have been synthesized by the combustion method using different fuels and oxidant sources. The use of maleic hydrazide and ammonium nitrate yields the formation of the undesirable $LiNb_3O_8$ second phase, as a consequence of the high exothermic reaction caused by these extra oxidant sources. The powder prepared by combustion method containing urea in excess produced high crystalline powders. Overall results reveal that the powders prepared by combustion methods showed superior sinterability than those prepared by solid-state reaction, as a simple consequence of its high surface area. In fact, powders synthesized by combustion can be used to produce polycrystalline $LiNbO_3$ powders at relatively low sintering temperatures, hence acting as an alternative approach to reduce the volatilization of the alkali ions during sintering.

Acknowledgement

We acknowledge the São Paulo Research Foundation for the financial support provided for this research.

References

[1] Rödel J, Jo W, Seifert K T P, Anton E M, Granzow T and Damjanovic D 2009 *J. Am. Ceram. Soc.* **92** 1153

[2] Jackson R A and Valerio M E G 2005 *J. Phys.*: *Condens. Matter* **17** 837

[3] Shrout T R and Zhang S J 2007 *J. Electroceram.* **19** 111

[4] Yin Q, Yuan S, Dong Q and Tian C 2010 *J. Alloys Compd.* **491** 340

[5] Rubio M F, Romero J J, Navarro R M G and Fernandez J F 2009 *J. Eur. Ceram. Soc.* **29** 3045

[6] Zhang B P, Li J F, Wang K and Zhang H 2006 *J. Am. Ceram. Soc.* **89** 1605

[7] Jaeger R E and Egerton L 1962 *J. Am. Ceram. Soc.* **45** 209

[8] Carlos S, Longo E, Leite E R and Varela J A 1996 *Mater. Lett.* **28** 215

[9] Liu M, Xue D and Luo C 2006 *J. Am. Ceram. Soc.* **89** 1551

[10] Kamali A R and Fray D J 2014 *Ceram. Int.* **40** 1835

[11] Kuo C L, Chen G J, Chang Y S, Fu J X, Chang Y H and Hwang W S 2012 *Ceram. Int.* **38** 3729

[12] Wood B D, Mocanu V and Gates B D 2008 *Adv. Mater.* **20** 4552

[13] Mokkelbost T, Kaus I, Grande T and Einarsrud M A 2004 *Chem. Mater.* **16** 5489

[14] Zeng H C and Tung S K 1996 *Chem. Mater.* **8** 2667

[15] Camargo E R and Kakihana M 2002 *Solid State Ion.* **151** 413

[16] Liu M, Xue D and Luo C 2006 *J. Alloys Compd.* **426** 118

[17] Wang L H, Yuan D R, Duan X L, Wang X Q and Yu F P 2007 *Cryst. Res. Technol.* **42** 321

[18] Cheng Z, Ozawa K, Miyazaki A and Kimura H 2005 *J. Am. Ceram. Soc.* **88** 1023

[19] An C, Tang K, Wang C, Shen G, Jin Y and Qian Y 2002 *Mater. Res. Bull.* **37** 1791

[20] Liu M, Xue D, Zhang S, Zhu H, Wang J and Kitamura K 2005 *Mater. Lett.* **59** 1095

[21] Patil K C, Aruna S T and Mimani T 2002 *Curr. Opin. Solid State Mater. Sci.* **6** 507

[22] Liu M and Xue D 2006 *Solid State Ion.* **177** 275

[23] Kuo C L, Chang Y S, Chang Y H and Hwang W S 2011 *Ceram. Int.* **37** 951

[24] Jain S R, Adiga K C and Pai V V R 1981 **40** 71

[25] Sousa V C, Segadães A M, Morelli M R and Kiminami R H G A 1999 *Int. J. Inorg. Mater.* **1** 235

[26] Segadães A M, Morelli M R and Kiminami R H G A 1997 *J. Eur. Ceram. Soc.* **132–136** 209

[27] Prakash A S, Manikandan P, Ramesha K, Sathiya M, Tarascon J M and Shukla A K 2010 *Chem. Mater.* **2857–2863** 22

[28] Jardiel T, Caballero A C, Marín-Dobrincic M, Cantelar E and Cussó F 2012 *Mater. Chem. Phys.* **676–680** 135

[29] Chiang W D, Birnie Y M and Kingery D P 1997 *Physical ceramics — principles for ceramic science and engineering* (New York: John Wiley)

[30] Brook R 1969 *J. Am. Ceram. Soc.* **52** 56